



Measurement of the WW production cross section with dilepton final states in $p\bar{p}$ collisions at $\sqrt{s} = 1.96$ TeV and limits on anomalous trilinear gauge couplings

The DØ Collaboration
URL <http://www-d0.fnal.gov>
(Dated: March 17, 2009)

We measure the WW production cross section in $p\bar{p}$ collisions at a center of mass energy of 1.96 TeV and set limits on the associated trilinear gauge couplings. The $WW \rightarrow \ell\nu\ell\nu$ ($\ell = e, \mu$) decay channels are considered in 1 fb^{-1} of data collected by the DØ detector at the Fermilab Tevatron Collider. The measured cross section is $\sigma(p\bar{p} \rightarrow WW) = 11.5 \pm 2.1$ (stat + syst) ± 0.7 (lumi) pb. Using $SU(2)_L \otimes U(1)_Y$ -conserving constraints, the one-dimensional 95% C.L. limits on trilinear gauge couplings for $\Lambda = 2$ TeV are $-0.54 < \Delta\kappa_\gamma < 0.83$, $-0.14 < \lambda_\gamma < 0.18$, and $-0.14 < \Delta g_1^Z < 0.30$.

Preliminary Results for Winter 2009 Conferences

The non-Abelian gauge group structure of the electroweak sector of the standard model (SM) predicts specific interactions between the γ , W , and Z bosons. Two triple gauge-boson coupling (TGC) vertices, $WW\gamma$ and WWZ , provide important contributions to the $p\bar{p} \rightarrow WW$ production cross section. A detailed study of W boson pair production probes this non-Abelian structure and may be sensitive to new physics that would enhance WW production, such as anomalous values of the TGCs or the production and decay of new particles such as the Higgs boson [1]. Studying WW production at the Fermilab Tevatron Collider provides an opportunity to explore \sqrt{s} energies higher than that available at CERN e^+e^- Collider (LEP), and Tevatron experiments have both measured the WW cross section and set TGC limits in the past [2–4]. In this note we present the most precise measurement of the WW production cross section in $p\bar{p}$ collisions to date and updated limits on non-SM $WW\gamma$ and WWZ couplings.

We examine WW production via the process $p\bar{p} \rightarrow W^+W^- \rightarrow \ell^+\nu\ell^-\bar{\nu}$ ($\ell = e, \mu$; allowing for intermediate τ states) and use charged lepton p_T distributions to study the triple gauge couplings. The decay of two W bosons into electrons or muons results in a pair of isolated, high- p_T , oppositely charged leptons and a large amount of \cancel{E}_T due to the escaping neutrinos. This analysis uses $p\bar{p}$ collisions at a center of mass energy of 1.96 TeV, as recorded by the D0 detector [5] at the Tevatron. A combination of single-electron (ee and $e\mu$) or single-muon ($\mu\mu$) triggers were used to collect the data, which correspond to integrated luminosities of $1104 \pm 67 \text{ pb}^{-1}$, $1072 \pm 65 \text{ pb}^{-1}$, and $1002 \pm 61 \text{ pb}^{-1}$ for the ee , $e\mu$, and $\mu\mu$ final states, respectively [6].

Electrons are identified in the calorimeter by their electromagnetic showers, which must occur within $|\eta| < 1.1$ or $1.5 < |\eta| < 3.0$, where $\eta = -\ln[\tan(\frac{\theta}{2})]$ and θ is the polar angle measured at the center of the detector. In the ee channel, at least one electron must satisfy $|\eta| < 1.1$. Electron candidates are required to be spatially matched to a track from the central tracking system, to be isolated from other energetic particles, and to have a shower shape consistent with that of an electromagnetic shower. Electron candidates are also required to satisfy a tight requirement on a multivariate electron discriminator which takes into account track quality, shower shape, calorimeter and track isolation, and E/p , where E is the calorimeter cluster energy and p is the track momentum. The transverse momentum (p_T) measurement of an electron is based on calorimeter energy information and track position.

Muons are reconstructed in the pseudorapidity region $|\eta| < 2.0$. They are required to be spatially matched to a track from the central tracking system and to have matched sets of wire and scintillator hits before and after the muon toroid. Detector support structure limits muon system coverage in the region $|\eta| < 1.1$ and $4.25 < \phi < 5.15$, where ϕ is the azimuthal angle, and in this region a single set of matched wire and scintillator hits is required. Additionally, muons must be isolated with respect to other central tracks and to energy in the calorimeter.

Missing transverse energy (\cancel{E}_T) is determined based on the calorimeter energy deposition distribution with respect to the primary vertex. The \cancel{E}_T is corrected for the electromagnetic or jet energy scale, as appropriate, and the p_T of muon candidates.

Signal acceptances and background processes are studied with a detailed Monte Carlo (MC) simulation based on PYTHIA [7] in conjunction with the CTEQ6L1 [8] parton distribution functions, with detector simulation carried out by GEANT [9]. The Z boson p_T spectrum in $Z \rightarrow \ell\ell$ MC events is adjusted to match that predicted by RESBOS [10].

For each final state, we require the highest p_T (leading) lepton to have $p_T > 25$ GeV, the trailing lepton to have $p_T > 15$ GeV, and the leptons to be of opposite charge. Both charged leptons are required to originate from the same vertex. The leptons are also required to have a minimum separation $\Delta\mathcal{R} = \sqrt{(\Delta\eta)^2 + (\Delta\phi)^2}$ of $\Delta\mathcal{R}_{ee} > 0.8$ in the ee channel or $\Delta\mathcal{R}_{e\mu/\mu\mu} > 0.5$ in the $e\mu$ and $\mu\mu$ channels, in order to prevent overlap of the lepton isolation cones.

Background processes for WW production include $Z/\gamma^* \rightarrow \ell\ell$, $t\bar{t}$, and W +jets production, multijet production, and other diboson production including WZ , $W\gamma$, and ZZ production. All of the background contributions except W +jets, $W\gamma$, and multijet production are estimated from the MC simulation. These three backgrounds are estimated from the data as described below.

After the initial event selection, the dominant background in each channel is $Z/\gamma^* \rightarrow \ell\ell$. Much of this background is removed by requiring $\cancel{E}_T > 45$ (ee), 20 ($e\mu$), or 35 ($\mu\mu$) GeV, since Z boson production has no escaping neutrinos. For the ee channel, we require $\cancel{E}_T > 50$ if $|M_Z - m_{ee}| < 6$ GeV to further reduce the Z boson background. An azimuthal separation requirement between the leptons is more effective at reducing Z boson backgrounds than an invariant mass requirement in events containing muons. The $e\mu$ channel requires $\cancel{E}_T > 40$ GeV if $\Delta\phi_{e\mu} > 2.8$, and the $\mu\mu$ channel requires $\Delta\phi_{\mu\mu} < 2.45$.

Mismeasurement of the muon momentum can lead to spurious \cancel{E}_T which is collinear with the muon direction. Especially in the $\mu\mu$ channel, mismeasurement of the muon momentum can allow Z boson events to satisfy the \cancel{E}_T requirement. To suppress these events in the $\mu\mu$ channel, we require that the track for each muon candidate include at least one silicon microstrip tracker hit, for better momentum resolution, and that the azimuthal angle between each muon and the direction of the \cancel{E}_T satisfies $|\cos(\Delta\phi_{E_T, \mu})| < 0.98$.

A second background is $t\bar{t}$ production followed by the leptonic decay of subsequent W bosons. This background can be suppressed by requiring $q_T = |\vec{p}_{T\ell^+} + \vec{p}_{T\ell^-} + \vec{\cancel{E}}_T| < 20$ (ee), 25 ($e\mu$), or 16 ($\mu\mu$) GeV. This quantity is the transverse momentum of the WW system and is expected to be small at the Tevatron. However, for $t\bar{t}$ production and other background processes, q_T can be large, so this variable is a powerful discriminant against these backgrounds.

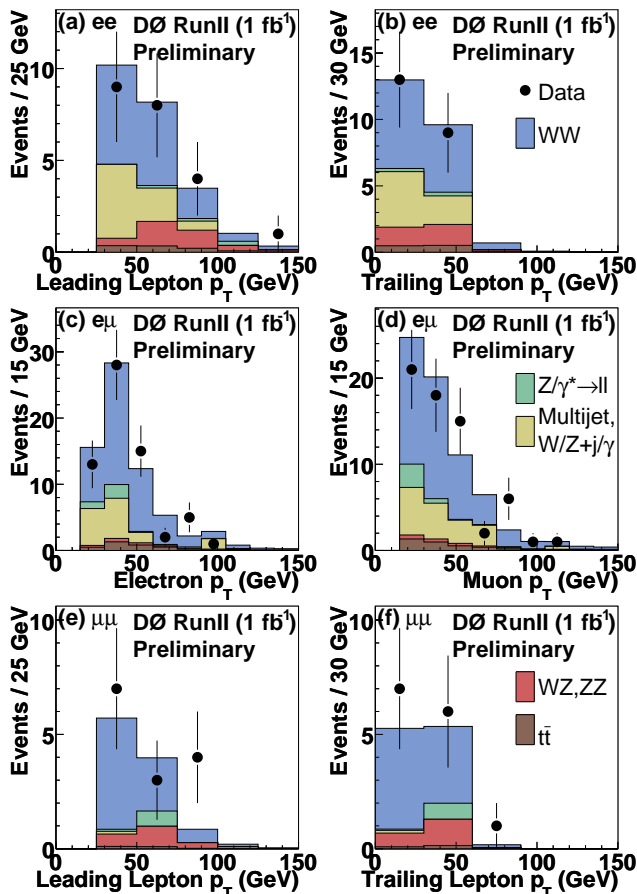


FIG. 1: Distributions of the (a) leading and (b) trailing electron p_T in the ee channel, (c) electron and (d) muon p_T in the $e\mu$ channel, and (e) leading and (f) trailing muon p_T in the $\mu\mu$ channel after final selection.

Another significant background is W +jet production in which the jet is misidentified as an electron or a muon. The probability for a jet to be misidentified as a lepton is determined from the data a special data sample by a tag and probe method. We select one jet which must be inconsistent with a lepton and require a second jet back-to-back in azimuth to the first. We also require that there be no high p_T leptons in the event to remove Z +jet events, and we require $\cancel{E}_T < 10$ GeV to remove W +jet events. The sample obtained in this way does not have significant Z boson contamination, as determined from the dijet invariant mass distribution. The second jet is the probe jet used to measure the jet misidentification probability.

The $W\gamma$ process is a background for only the ee and $e\mu$ channels, since a photon is not easily misidentified as a muon. We determine the probability that a photon is misidentified as an electron with photons from $Z/\gamma^* \rightarrow ee\gamma$ decays and adjust the $W\gamma$ MC to reflect that misidentification rate. The W +jets background is determined from the data by selecting dilepton samples with loose and tight lepton requirements and setting up a system of linear equations to solve for the W +jet backgrounds after all event selection.

The background due to multijet production, in which both lepton candidates are due to a jet which is misidentified as a lepton, is determined from the data using a sample of like-signed reconstructed objects that satisfy inverted lepton quality cuts. This background is labeled multijet in Fig. 1 and Table I.

The leptonic decay of WZ and ZZ events can mimic the WW signal when one or more of the charged leptons are not reconstructed and instead contribute to \cancel{E}_T . The $ZZ \rightarrow \ell\nu\nu$ process is suppressed in the same manner as $Z/\gamma^* \rightarrow \ell\ell$ decays.

For each channel, the exact values of selection requirements are chosen by performing a grid search on signal MC and expected background, minimizing the combined statistical and systematic uncertainty on the expected cross section measurement. For each final state, two contributions to the WW production signal are considered, both the prompt decay of the W bosons into the final state e or μ and the prompt decay of either W boson into a tau lepton with secondary decays that lead to the final state e or μ . The final lepton p_T distributions are shown in Fig. 1(a-f).

TABLE I: Numbers of signal and background events expected and number of events observed after the final event selection in each channel. Uncertainties include contributions from statistics and object selection efficiency. Negligible contributions are not shown.

Process	ee	$e\mu$	$\mu\mu$
$WW \rightarrow \ell\ell$	10.98 ± 0.59	39.25 ± 0.81	7.18 ± 0.34
$WW \rightarrow \ell\tau \rightarrow \ell\ell$	1.40 ± 0.20	5.18 ± 0.29	0.71 ± 0.10
$Z/\gamma^* \rightarrow ee/\mu\mu + X$	0.27 ± 0.20	2.52 ± 0.56	0.76 ± 0.36
$Z/\gamma^* \rightarrow \tau\tau$	0.26 ± 0.05	3.67 ± 0.46	—
$t\bar{t}$	1.10 ± 0.10	3.79 ± 0.17	0.22 ± 0.04
WZ	1.42 ± 0.14	1.29 ± 0.14	0.97 ± 0.11
$W\gamma$	0.23 ± 0.16	5.21 ± 2.97	—
ZZ	1.70 ± 0.04	0.09 ± 0.01	0.84 ± 0.03
$W + \text{jet}$	6.09 ± 1.72	7.50 ± 1.83	0.12 ± 0.24
Multijet	0.01 ± 0.01	0.14 ± 0.13	—
Background sum	11.07 ± 1.75	24.21 ± 3.58	2.91 ± 0.45
Data	22	64	14

The overall detection efficiency for $W^+W^- \rightarrow e^+\nu_e e^-\bar{\nu}_e$ is $(7.18 \pm 0.39)\%$, while that for $W^+W^- \rightarrow e\tau/\tau\tau + \nu\bar{\nu} \rightarrow e^+e^- + \nu\bar{\nu}$ is $(2.24 \pm 0.32)\%$. The overall detection efficiency for $W^+W^- \rightarrow e^\pm\nu_e\mu^\mp\nu_\mu$ is $(13.43 \pm 0.28)\%$, while that for $W^+W^- \rightarrow e\tau/\mu\tau/\tau\tau + \nu\bar{\nu} \rightarrow e^\pm\mu^\mp + \nu\bar{\nu}$ is $(4.36 \pm 0.24)\%$. The overall detection efficiency for $W^+W^- \rightarrow \mu^+\nu_\mu\mu^-\bar{\nu}_\mu$ is $(5.34 \pm 0.25)\%$, while that for $W^+W^- \rightarrow \mu\tau/\tau\tau + \nu\bar{\nu} \rightarrow \mu^+\mu^- + \nu\bar{\nu}$ is $(1.30 \pm 0.18)\%$.

The numbers of estimated signal and background events and the number of observed events for each channel after the final event selection are summarized in Table I. Assuming the W boson and τ branching ratios from [11], the observations in data correspond to $\sigma(p\bar{p} \rightarrow WW) = 10.6 \pm 4.6$ (stat) ± 1.9 (syst) ± 0.7 (lumi) pb in the ee channel, $10.8 \pm 2.2 \pm 1.1 \pm 0.7$ pb in the $e\mu$ channel, and $16.9 \pm 5.7 \pm 1.0 \pm 1.0$ pb in the $\mu\mu$ channel. The most significant sources of systematic uncertainty for each channel are the statistics associated with the estimation of the $W + \text{jet}$ contribution in the ee channel, the photon misidentification probability used to estimate the $W\gamma$ contribution in the $e\mu$ channel, and the MC statistics for backgrounds in the $\mu\mu$ channel.

The decay channels are combined using the best linear unbiased estimate (BLUE) method [12], and the cross section corresponding to the combined observations across all three final states is $\sigma(p\bar{p} \rightarrow WW) = 11.5 \pm 2.1$ (stat + syst) ± 0.7 (lumi) pb. This measured cross section is consistent with the most recent published result from the Tevatron, $11.8^{+3.7}_{-3.3}$ (stat) $^{+1.0}_{-0.8}$ (syst) ± 0.6 (lumi) pb [2]. Standard model calculations of the WW production cross section at this center of mass energy range from 13 to 13.5 pb [13].

The triple gauge couplings that govern WW production can be parameterized by a general Lorentz-invariant Lagrangian with fourteen independent complex coupling parameters, seven each for the $WW\gamma$ and WWZ vertices [1]. Limits on the anomalous couplings are often obtained by taking the parameters to be real, enforcing electroweak gauge invariance, and assuming charge conjugation and parity invariance, reducing the number of independent couplings to five: g_1^Z , κ_Z , κ_γ , λ_Z , and λ_γ . In the SM, $g_1^Z = \kappa_Z = \kappa_\gamma = 1$ and $\lambda_Z = \lambda_\gamma = 0$. The couplings that are non-zero in the SM are often written in terms of their deviation from the SM values, for example $\Delta g_1^Z \equiv g_1^Z - 1$, a convention we follow here. Enforcing $SU(2)_L \otimes U(1)_Y$ symmetry introduces two relationships between the remaining parameters: $\kappa_Z = g_1^Z - (\kappa_\gamma - 1)\tan^2\theta_W$ and $\lambda_Z = \lambda_\gamma$, further reducing the number of free parameters to three [14].

One effect of introducing anomalous coupling parameters into the SM Lagrangian is an enhancement of the cross section for the $q\bar{q} \rightarrow Z/\gamma^* \rightarrow W^+W^-$ process, an effect which leads to unphysically large cross sections at high energy. Therefore, the anomalous couplings must vanish as $s \rightarrow \infty$. This is achieved by introducing a dipole form factor for an arbitrary coupling α (g_1^Z , κ_V , or λ_V): $\alpha(\hat{s}) = \alpha_0/(1 + \hat{s}/\Lambda^2)^2$, where \hat{s} is the partonic center of mass energy, the form factor scale Λ is set by new physics, and limits are set in terms of α_0 . Unitarity constraints provide an upper limit for each coupling that is dependent on the choice of Λ . For this analysis we use $\Lambda=2$ TeV, the approximate center of mass energy of the Tevatron.

The leading order MC event generator by Hagiwara, Woodside, and Zeppenfeld [1] is used to model the behavior of the WW system as coupling parameters are varied about their SM values. A grid of points in three-dimensional $(\Delta\kappa_\gamma, \lambda_\gamma, \Delta g_1^Z)$ space is generated to define the behavior of the anomalous WW system. The events generated for each grid point are passed through a parameterized simulation of the D0 detector that is tuned to data.

Since the rest frame of the WW system cannot be reconstructed, the p_T s of the charged leptons are used to test the triple gauge couplings. To enhance the sensitivity to anomalous couplings, events are binned two-dimensionally in lepton p_T , using leading and trailing lepton p_T values in the ee and $\mu\mu$ channels, and electron and muon p_T values in

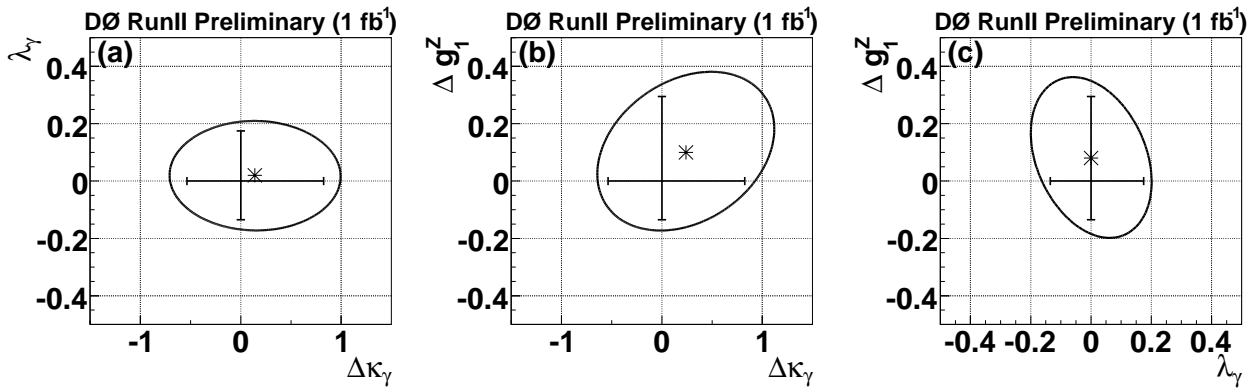


FIG. 2: One and two-dimensional 95% C.L. limits when enforcing $SU(2)_L \otimes U(1)_Y$ symmetry at $\Lambda = 2$ TeV, for (a) $\Delta\kappa_\gamma$ vs. λ_γ , (b) $\Delta\kappa_\gamma$ vs. Δg_1^Z , and (c) λ_γ vs. Δg_1^Z , each when the third free coupling is set to its SM value. The curve represents the two-dimensional 95% C.L. contour and the ticks along the axes represent the one-dimensional 95% C.L. limits. An asterisk (*) marks the point with the highest likelihood in the two-dimensional plane.

the $e\mu$ channel. For each bin in lepton p_T space, the expected number of WW events produced is parameterized by a quadratic function in the three-dimensional $(\Delta\kappa_\gamma, \lambda_\gamma, \Delta g_1^Z)$ space. Coupling parameters are investigated in pairs, with the third parameter fixed to the SM value. A likelihood surface is generated by considering all channels simultaneously, integrating over the signal, background, and luminosity uncertainties with Gaussian distributions in a similar method as that used in previous studies [4].

The one-dimensional 95% C.L. limits for $\Lambda = 2$ TeV are determined to be $-0.54 < \Delta\kappa_\gamma < 0.83$, $-0.14 < \lambda_\gamma < 0.18$, and $-0.14 < \Delta g_1^Z < 0.30$. One- and two-dimensional 95% C.L. limits are shown in Fig. 2.

The combined anomalous coupling limits from the LEP collaborations are more stringent and independent of Λ [15]. The limits obtained here are complementary in that they use hadronic collisions at the Tevatron and explore a range of parton center of mass energies that include values of \sqrt{s} exceeding the LEP kinematic limit of 208 GeV.

In summary, we have measured the WW production cross section using 1 fb^{-1} of data at the D0 experiment. We measure a cross section of $\sigma(p\bar{p} \rightarrow WW) = 11.5 \pm 2.1$ (stat + syst) ± 0.7 (lumi) pb, the most precise measurement of the WW cross section at a hadronic collider to date. The selected event kinematics are used to set limits on anomalous values of the electroweak triple gauge couplings.

-
- [1] K. Hagiwara, J. Woodside, and D. Zeppenfeld, Phys. Rev. D **41**, 2113 (1990); K. Hagiwara, R. D. Peccei, D. Zeppenfeld, Nucl. Phys. **B282**, 253 (1987).
 - [2] V. M. Abazov *et al.* (D0 Collaboration), Phys. Rev. Lett. **94**, 151801 (2005); V. M. Abazov *et al.* (D0 Collaboration), Phys. Rev. Lett. **100**, 139901(E) (2008).
 - [3] D. Acosta *et al.* (CDF Collaboration), Phys. Rev. Lett., **94**, 211801 (2005).
 - [4] V. M. Abazov *et al.* (D0 Collaboration), Phys. Rev. D **74**, 057101 (2006).
 - [5] V. M. Abazov *et al.* (D0 Collaboration), Nucl. Instrum. Methods Phys. Res. A **565**, 463 (2006).
 - [6] T. Andeen *et al.*, Fermilab Report No. FERMILAB-TM-2365, 2007. A 6.1% uncertainty is assigned to the integrated luminosity measurement.
 - [7] H. U. Bengtsson and T. Sjöstrand, Comput. Phys. Commun. **46**, 43 (1987); T. Sjöstrand *et al.*, Comp. Phys. Comm., **135**, 283 (2001). We use PYTHIA v6.319.
 - [8] J. Pumplin *et al.*, J. High Energy Phys. **07**, 012 (2002).
 - [9] S. Agostinelli *et al.*, Nucl. Inst. Methods Phys. Res. A **506**, 250 (2003).
 - [10] C. Balazs and C. P. Yuan, Phys. Rev. D **56**, 5558 (1997).
 - [11] C. Amsler *et al.*, Phys. Lett. B **667**, 1 (2008).
 - [12] P. Clifford, D. Gibaut, and L. Lyons, Nucl. Inst. Methods Phys. Res. A **270** 110 (1998).
 - [13] J. M. Campbell and R. K. Ellis, Phys. Rev. D **60**, 113006 (1999).
 - [14] A. De Rújula, M. B. Gavela, P. Hernandez and E. Masso, Nucl. Phys. **B384**, 3 (1992).
 - [15] S. Schael *et al.* (ALEPH Collaboration), Phys. Lett. B **614**, 7 (2005); P. Achard *et al.* (L3 Collaboration), Phys. Lett. B **586**, 151 (2004); G. Abbiendi *et al.* (OPAL Collaboration), Eur. Phys. J. C **33**, 463 (2004).